Transport properties of CO_2-expanded acetonitrile from molecular dynamics simulations

Yao Houndonougbo
Center for Environmentally Beneficial Catalysis, University of Kansas, Lawrence, Kansas 66045

Brian B. Laird
Center for Environmentally Beneficial Catalysis, University of Kansas, Lawrence, Kansas 66045 and Department of Chemistry, University of Kansas, Lawrence, Kansas 66045

Krzysztof Kuczera[a)]
Center for Environmentally Beneficial Catalysis, University of Kansas, Lawrence, Kansas 66045; Department of Chemistry, University of Kansas, Lawrence, Kansas 66045; and Department of Molecular Biosciences, University of Kansas, Lawrence, Kansas 66045

(Received 18 October 2006; accepted 28 December 2006; published online 21 February 2007)

Carbon-dioxide-expanded liquids, which are mixtures of organic liquids and compressed CO_2, are novel media used in chemical processing. The authors present a molecular simulation study of the transport properties of liquid mixtures formed by acetonitrile and carbon dioxide, in which the CO_2 mole fraction is adjusted by changing the pressure, at a constant temperature of 298 K. They report values of translational diffusion coefficients, rotational correlation times, and shear viscosities of the liquids as function of CO_2 mole fraction. The simulation results are in good agreement with the available experimental data for the pure components and provide interesting insights into the largely unknown properties of the mixtures, which are being recognized as important novel materials in chemical operations. We find that the calculated quantities exhibit smooth variation with composition that may be represented by simple model equations. The translational and rotational diffusion rates increase with CO_2 mole fraction for both the acetonitrile and carbon dioxide components. The shear viscosity decreases with increasing amount of CO_2, varying smoothly between the values of pure acetonitrile and pure carbon dioxide. Our results show that adjusting the amount of CO_2 in the mixture allows the variation of transport rates by a factor of 3–4 and liquid viscosity by a factor of 8. Thus, the physical properties of the mixture may be tailored to the desired range by changes in the operating conditions of temperature and pressure. © *2007 American Institute of Physics*. [DOI: 10.1063/1.2434968]

INTRODUCTION

Carbon-dioxide-expanded liquids (CXLs), formed by adding compressed CO_2 to standard organic solvents, are a novel class of media for chemical processing. CXLs have intermediate properties between pure organic solvents and supercritical CO_2. The use of standard organic solvents allows the optimization of catalyst solubilty, while causing concerns with toxicity and vapor emissions which may be toxic and form explosive mixtures in air. On the other hand, the use of supercritical CO_2 as solvent, while favorable from the point of view of pollution prevention, has drawbacks in the form of the low solubility of catalysts and the economic costs of operation at high pressures with low reaction rates. CXLs are a compromise between organic liquids and supercritical CO_2. From the processing standpoint, catalyst and reactant solubilities are sufficient to yield relatively high reaction rates. Replacement of part of the organic liquid by the benign CO_2 decreases the environmental concerns compared to organic solvents, while faster reaction rates and lower operating pressures improve the economic performance compared to supercritical CO_2. Additionally, adjusting the system pressure allows for smooth changes in CO_2 content and thus also in physical properties of the liquids.

In recent years a significant research effort has been undertaken to evaluate the efficacy of CXLs as novel media for chemical processing.[1–3] Studies of CXL-based chemical reactions are a major component of the investigations at the Center for Environmentally Benign Catalysis (CEBC) at the University of Kansas. Recent CEBC contributions include studies of several catalytic processes in CO_2 expanded solvents,[4–7] as well as modeling of the vapor-liquid equilibria of several CO_2-expanded organic liquids.[8]

In this paper we continue our studies of CO_2-expanded organic liquids, presenting results of simulations of transport properties for a series of CO_2-acetonitrile mixtures of varying composition. We use previously published potential energy functions of CO_2 (Ref. 9) and acetonitrile[10] to generate nanosecond length molecular dynamics trajectories of the pure components and their mixtures. We calculate translational diffusion coefficients and rotational correlation times for both components as a function of CO_2 mole fraction. Our results indicate that the transport properties of CO_2-expanded acetonitrile may be varied in a smooth, predictable manner

[a)]Tel: (785)-864-5060. Fax: (785)-864-5396. Electronic mail: kkuczera@ku.edu

by adjusting the pressure of the CO_2 component. We also compare our results with those of Li and Maroncelli, who recently reported simulations of transport properties for CO_2-acetonitrile mixtures using a different potential for CH_3CN and different simulation conditions.[11]

The molecular models and computational methods are described in *Methods*, the results are described in *Results and Discussion*, and final conclusions are presented in *Conclusions*.

METHODS

CO_2 model

The carbon dioxide model was adapted from the three-site EPM model developed by Harris and Yung.[9] The Lennard-Jones parameters and equilibrium C–O bond lengths (r_0=1.149 Å) were taken directly from Harris and Yung.[9] In the original paper a harmonic term $\frac{1}{2}k_\theta(\theta-\theta_0)^2$, with θ as the O–C–O angle, was used to describe the potential energy of CO_2 bending, with k_θ=305 kcal/(mol rad^2) and $\theta_0=\pi$ radians as the equilibrium angle. In our simulations we added a harmonic energy term to describe bond stretching $\frac{1}{2}k_{CO}(r-r_0)^2$, with r as the C–O distance. For our flexible model the values of the two force constants, k_θ =58 kcal/(mol rad^2) and k_{CO}=1150 kcal/(mol A^2) were taken directly from the optimized vibrational force field of Suzuki.[12] These force constants yielded vibrational frequencies of 2492, 1302, and 682 cm^{-1}, for the asymmetric stretch, symmetric stretch, and bending modes, respectively, as calculated with the MOLVIB module of the program CHARMM.[13] Given our highly simplified two-parameter vibrational force field, this is in reasonable agreement with the corresponding observed gas phase values of 2349, 1388, and 667 cm^{-1}, respectively.[12] In our simulations we used the standard Berthelot combination rules for the Lennard-Jones parameters, rather than the modified rules introduced by Harris and Yung.[9] The same rules were employed for all atom pairs in the pure liquids and mixtures simulated here, allowing for a consistent and simple treatment of all these systems.

The motivation for introducing flexibility into the CO_2 model was twofold. First, this simple modification leads to a more physically realistic model, which may be consistently extended for use with other organic solvents. Second, preliminary simulations with the rigid bond model using the CHARMM program indicated the need for a 1 fs molecular dynamics (MD) time step in order to generate stable trajectories. This was due to the inefficiency of the SHAKE algorithm used to enforce bond constraints.[14] With the flexible force field MD simulations were more efficient, as stable unconstrained trajectories could easily be generated with a 2 fs time step, producing savings both due to the doubling of time step and elimination of SHAKE use.

Acetonitrile model

The acetonitrile model was adopted from the three-site GROMOS model developed by Hirata.[10] The Lennard-Jones parameters and equilibrium C–C and C–N bond lengths (1.46 and 1.17 Å, respectively) were taken directly from Hirata.[10] Analogous to our CO_2 calculations, we defined a flexible force field for the acetonitrile model, by introducing three harmonic force constants, k_{CC}, k_{CN}, and k_θ, describing C–C bond stretching, C–N bond stretching, and C–C–N bending, respectively. Initial values of the force constants were taken from the empirical force field based on gas-phase vibrations.[15] The final values of the force constants, k_{CC} =380 kcal/(mol Å^2), k_{CN}=1280 kcal/ mol Å^2), and k_θ =20 kcal/(mol rad^2), were obtained by optimizing the fit between the vibrational frequencies calculated within our three-point model and the subset of the corresponding observed vibrational frequencies of gaseous CH_3CN, using the MOLVIB module of CHARMM.[13] The optimized force constants yielded CH_3CN vibrational frequencies of 2272, 922, and 364 cm^{-1}, for the C–N stretch, C–C stretch, and C–C–N bending modes, respectively. This was in excellent agreement with the corresponding observed values of 2267, 920, and 362 cm^{-1}.[15]

System preparation

For each simulated system, a cubic box with 512 molecules was prepared. For the pure liquids initial structures were generated by placing randomly oriented molecules on an $8\times8\times8$ grid with 5 Å spacing. For mixtures with desired CO_2 mole fraction x an $11\times11\times11$ grid with 5 Å spacing was filled with randomly oriented molecules, with the type of molecule selected at random; CO_2 has probability x and the cosolvent acetonitrile has probability $1-x$. A system of desired composition, e.g., with 51 CO_2 and 461 acetonitriles for x=0.1, was then carved out of this larger box using CHARMM. Each system was prepared by a cycle of energy minimizations and constant pressure molecular dynamics simulations of total length of 1 ns, starting with an exaggerated cubic box size of side a=40 Å and leading to an equilibrated cubic box at 298 K and desired target pressure (see Table I). The pure CO_2 system was the exception, for which a 2 ns equilibration was needed to reach a state with stable density. The final structures from these equilibrations were employed as the starting points for 1 ns constant pressure (*NPT*) simulations. To create starting coordinates for constant volume (*NVT*) simulations, the *NPT* equilibrated structures of our systems were subjected to two stages of 500 ps constant volume MD, the first with a density intermediate between the target value and the one found in the constant pressure trajectory, and the second at the desired target value, corresponding to the experimental density. The basic thermodynamic parameters of the simulated systems are described in Table I. For pure acetonitrile, the target pressure was 1 bar in the *NPT* simulation and the target density d =0.776 g/cm^3 (the experimental density at 298 K and 1 bar[16]) for the *NVT* case. Analogously, for pure CO_2 the target pressure was p=64 atm for *NPT* and target density d =0.7301 g/cm^3 for *NVT*, which correspond to the experimental conditions for liquid phase in equilibrium with its vapor at 298 K. For the mixtures, values of target pressure and density were obtained by linear interpolation from measurements of Kordikowski *et al.*[17]

TABLE I. Conditions for CO_2-acetonitrile mixture simulations at 298 K. For *NPT* simulations the target pressures P and average densities d and cubic cell sizes a are given, for *NVT* simulations the actual densities and cell sizes. CO_2 mole fractions: x; number of CO_2 molecules: N_{CO_2}; number of acetonitrile molecules: N_{acnt}.

System			*NPT*			*NVT*	
x	N_{CO_2}	N_{acnt}	P (atm)	d (g/cm^3)	a (Å)	d (g/cm^3)	a (Å)
0.00	0	512	1.0	0.7155±0.0015	36.54±0.03	0.776	35.56
0.10	51	461	4.0	0.7335±0.0017	36.32±0.03	0.786	35.50
0.20	102	410	12.0	0.7549±0.0021	36.06±0.04	0.812	35.20
0.30	154	358	20.0	0.7800±0.0037	35.76±0.06	0.835	34.95
0.40	205	307	26.0	0.7969±0.0016	35.58±0.03	0.865	34.74
0.50	256	256	33.0	0.8144±0.0035	35.41±0.06	0.870	34.64
0.60	307	205	40.0	0.8312±0.0057	35.25±0.09	0.889	34.47
0.70	358	154	48.0	0.8286±0.0028	35.37±0.04	0.897	34.45
0.80	102	410	52.0	0.8205±0.0072	35.57±0.11	0.893	34.58
0.90	410	102	55.0	0.8043±0.0162	35.88±0.24	0.878	34.85
1.00	512	0	64.0	0.7819±0.0094	36.31±0.15	0.713	37.44

Molecular dynamics simulations

For each system listed in Table I, 1 ns MD simulations were carried out under two kinds of conditions—constant volume (*NVT*) and constant pressure (*NPT*). The Nosé-Hoover algorithm was used to maintain a constant temperature of 298 K in all cases,[18] while the Langevin piston method was used to maintain constant pressure in the *NPT* trajectories.[19] This method has been found to eliminate problems with unphysical energy distributions which may occur if weak coupling is employed.[19] For van der Waals nonbonded interactions, modeled by the Lennard-Jones 6-12 potential, an atom-based 12.0 Å nonbonded cutoff distance was employed, with a switching function between 10.0 and 12.0 Å. To avoid truncation effects, the particle-mesh Ewald method was used for electrostatic interactions, with roughly 1 Å grid spacing and parameter $\kappa=0.34$ Å^{-1}.[20] For acetonitrile, CO_2, and their mixtures a 2 fs integration time step was employed without the use of SHAKE constraints. Simulations were performed on 46-CPU Xeon Linux cluster at the Center for Environmentally Beneficial Catalysis at the University of Kansas, using the program CHARMM version 30.[13] Typically, a 1 ns simulation required about 8 h of simulation on one processor.

Calculation of transport properties

The translational diffusion coefficients D_t of the molecules were calculated based on the expression[21]

$$D_t = \lim_{t\to\infty} \frac{\langle \Delta r^2(t)\rangle}{6t}, \tag{1}$$

where $\Delta r(t)$ is the displacement of the center of mass in time t and $\langle \ldots \rangle$ denotes an average over starting times and all molecules of a given type. The values of D_t were obtained by fitting to a straight line the center-of-mass displacements corrected for effects of the periodic boundary conditions, over a time range of 50–500 ps, where the $\Delta r^2(t)$ plots tended to be linear.

To obtain a description of rotational dynamics that may be related to experimental measurements, we calculated the second order correlation functions,

$$C_2(t) = \langle 3(\mathbf{n}(0)\cdot\mathbf{n}(t))^2 - 1\rangle/2, \tag{2}$$

where $\mathbf{n}(t)$ is the direction of the molecular axis at time t and the averaging is performed over starting structures and all molecules of a given type. The correlation functions were fitted to single-exponential decays, yielding the second-order rotational correlation times τ.[22,23] The molecular axes were taken to be unit vectors along the line between the two end atoms of CO_2 and acetonitrile, respectively. In the rotational diffusion model, in which it is assumed that molecular reorientations occur in small independent steps, the correlation times τ may be expressed in terms of components of the rotational diffusion tensor.[22,23] Within our models, both CO_2 and acetonitrile are linear molecules, and in that case their reorientations are described by a single rotational diffusion coefficient D_r, related to the correlation time by $\tau=1/6D_r$.

The viscosity calculations were based on the Green-Kubo formula, involving integrals of the autocorrelation functions (ACFs) of the off-diagonal elements of the stress tensor $J_{\alpha\beta}$,[24] e.g.,

$$\eta_{xy} = \frac{1}{kTV}\int_0^\infty \langle J_{xy}(0)J_{xy}(t)\rangle dt, \tag{3}$$

with V as the system volume, k as the Boltzmann constant, and T as the temperature. The contributions from xy, xz, and yz components were averaged. For viscosity calculations, the existing *NVT* trajectories were extended by 500 ps, with coordinates and velocities saved every 2 fs and stress tensor components evaluated with CHARMM. The calculated autocorrelation functions exhibited fast fluctuations, changing sign with a period of 20–40 fs. The time integrals were evaluated up to a correlation time τ_J, after which it was assumed that the autocorrelation function fluctuations represent random noise. The correlation times were estimated as the point at which the magnitude of the ACFs fell to about 1% of their initial values. These values ranged from about 11 ps for

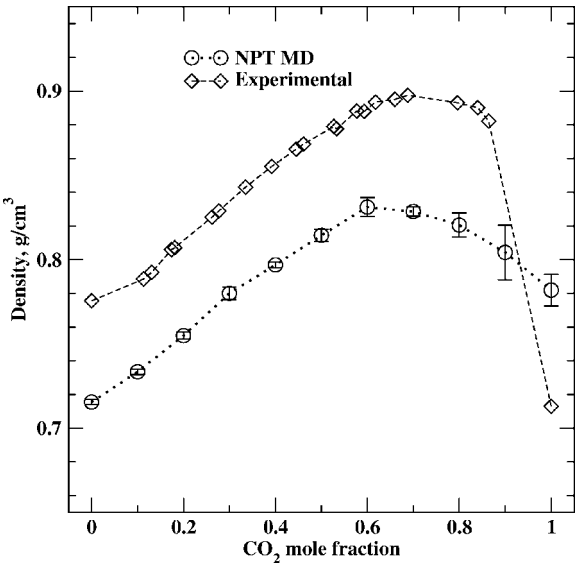

FIG. 1. Comparison of calculated and experimental densities in CO_2-acetonitrile mixtures. Squares—measurements,[7] circles—*NPT* MD simulation results.

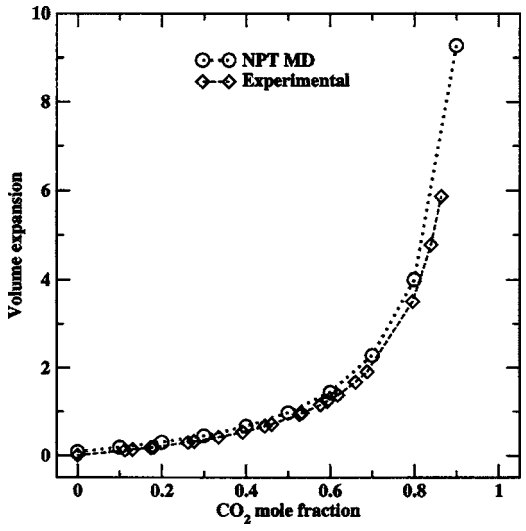

FIG. 2. Comparison of calculated and experimental volume expansions in CO_2-acetonitrile mixtures. Squares—measurements,[17] circles—*NPT* MD simulation results.

pure acetonitrile to 3 ps for pure CO_2. Extending the integration by a factor of 2 beyond these τ_J typically led to changes in viscosity values of 10%–20%.

Error estimates

Mean values of the calculated physical quantities, densities, translational diffusion coefficients, rotational correlation times, and shear viscosities were evaluated over the full 1 ns MD trajectories. To estimate statistical errors of the means, each trajectory was divided into five consecutive fragments (blocks). Values calculated from the fragments were used to obtain a standard deviation of the mean s_b, equal to $s/\sqrt{5}$, with s as the standard deviation of the sample of five block data points. The reported errors are equal to $2.57s_b$, i.e., they represent the 95% confidence interval of the t distribution for five degrees of freedom.

RESULTS AND DISCUSSION

Density and volume expansion

As a test of the model, we have calculated the liquid densities from the constant pressure simulations for the pure components and their mixtures (Table I, Fig. 1). The calculated density of pure acetonitrile, 0.716(2) g cm^3, is underestimated by about 8% compared to the experimental value of 0.776 g cm^{-3} at 298 K and 1 bar.[16] In turn, the calculated density of pure CO_2, 0.782(1) g cm^{-3}, is overestimated by about 10% compared to the experimental value of 0.713 g cm^{-3} at 298 K and 63.5 bars.[25,26] The calculated value is in accord with the 0.7772(6) g cm^{-3} found in the Gibbs-ensemble Monte Carlo simulations of Harris and Yung using the unmodified EPM potential.[9]

The densities of the acetonitrile-CO_2 mixtures tend to be lower than the experimental values, with underestimates in the range of 6%–8%. Interestingly, the density maximum reached at compositions of 0.6–0.7 CO_2 mole fraction is reproduced by the simulation results. A similar trend in the variation of density with composition was found by Li and Maroncelli, although these authors obtained better agreement of liquid densities with experimental data due to choice of a different potential energy for acetonitrile.[11]

The calculated volume expansions of the CO_2-acetonitrile mixtures are presented in Fig. 2. The calculated results are highly similar to the experimental data.

Translational diffusion

The calculated translational diffusion coefficients D_t are presented in Table II and Fig. 3. Experimental measurements for pure acetonitrile give $D_t=0.43\times10^{-8}$ m^2/s.[27] Our *NPT* trajectory predicts a value of $0.47(1)\times10^{-8}$ m^2 s^{-1} at 298 K and 1 bar, while the *NVT* yields $0.33(1)\times10^{-8}$ m^2 s^{-1} at 298 K and experimental density. These results are consistent with previous calculations of Hirata, who obtained $D_t=0.44(2)\times10^{-8}$ m^2 s^{-1} at a slightly higher density of 0.79 g/cm^3.[10] For pure CO_2, the measured value at 298 K and 68 bars, the thermodynamic point closest to our simulation conditions, is $D_t=2.18\times10^{-8}$ m^2 s^{-1}.[28] The calculations

TABLE II. Calculated translational diffusion coefficients in CO_2-acetonirile mixtures at 298 K. Units: 10^{-8} m^2 s^{-1}. x is the CO_2 mole fraction.

	CO_2		Acetonitrile	
x	*NPT*	*NVT*	*NPT*	*NVT*
0.00	⋯	⋯	0.47±0.01	0.33±0.01
0.10	0.69±0.04	0.51±0.02	0.50±0.01	0.38±0.01
0.20	0.71±0.02	0.55±0.02	0.52±0.02	0.40±0.01
0.30	0.73±0.04	0.56±0.02	0.54±0.02	0.41±0.01
0.40	0.79±0.04	0.61±0.02	0.59±0.02	0.44±0.02
0.50	0.80±0.01	0.68±0.01	0.59±0.01	0.50±0.01
0.60	0.89±0.04	0.72±0.02	0.66±0.03	0.53±0.02
0.70	1.02±0.02	0.83±0.03	0.74±0.01	0.61±0.02
0.80	1.17±0.05	0.94±0.03	0.85±0.05	0.70±0.01
0.90	1.33±0.11	1.12±0.03	0.96±0.06	0.86±0.03
1.00	1.54±0.04	1.76±0.04	⋯	⋯

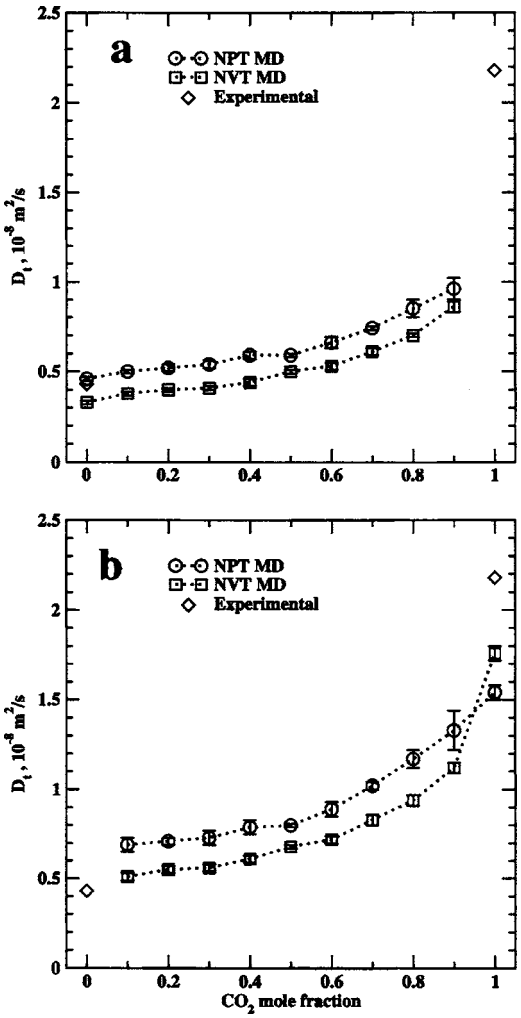

FIG. 3. Translational diffusion coefficients in CO_2-acetonitrile mixtures. Units are $Å^2\,ps^{-1}=10^{-8}\,m^2\,s^{-1}$. (a) Calculated values for acetonitrile: circles—*NPT*, squares—*NVT* MD. (b) Calculated values for CO_2: circles—*NPT*, squares—*NVT* MD. Diamonds: Experimental values for pure acetonitrile at 1 bar and 298 K (Ref. 27) and for pure CO_2 at 64 atm and 298 K (Ref. 28).

predict coefficients of 1.54×10^{-8} m^2 s^{-1} (*NPT* at 298 K and 64 bars) and 1.76×10^{-8} m^2 s^{-1} (*NVT* at 298 K and experimental density). The deviations between the experimental and calculated results are significantly larger than the statistical errors of the former and fall into the 7%–30% range. This level of agreement is typical for cases when transport properties were not used to optimize the model parameters. We expect that this should be sufficient for us to make reliable predictions about changes in D_t with composition.

There is a clear trend in the results, with translational diffusion rates of both CO_2 and acetonitrile increasing with increasing CO_2 mole fraction x_{CO_2}. This effect may be rationalized based on the D_t of the pure liquids, such that adding the more mobile CO_2 to the liquid phase speeds up translation of acetonitrile, while the CO_2 motions themselves are slowed down by collisions with the less mobile acetonitrile. Overall, our simulations predict that the rate of translational diffusion in CO_2-acetonitrile mixtures may be varied by a factor of 2–4 by changing the CO_2 content. The trends found by Li and Maroncelli were similar, with translation diffusion

TABLE III. Calculated rotational correlation times in CO_2-acetonitrile mixtures at 298 K. Units: ps. x is the CO_2 mole fraction.

	CO_2		Acetonitrile	
x	*NPT*	*NVT*	*NPT*	*NVT*
0.00	⋯	⋯	1.19±0.06	1.45±0.02
0.10	0.63±0.02	0.74±0.03	1.09±0.03	1.33±0.02
0.20	0.58±0.01	0.68±0.02	1.06±0.04	1.28±0.01
0.30	0.57±0.02	0.66±0.03	1.06±0.05	1.25±0.02
0.40	0.55±0.02	0.61±0.02	1.00±0.06	1.22±0.02
0.50	0.52±0.02	0.57±0.01	1.00±0.03	1.14±0.02
0.60	0.48±0.02	0.53±0.01	0.94±0.04	1.09±0.03
0.70	0.43±0.02	0.48±0.02	0.91±0.02	0.99±0.02
0.80	0.38±0.01	0.42±0.02	0.86±0.04	0.95±0.02
0.90	0.34±0.02	0.36±0.01	0.80±0.07	0.82±0.03
1.00	0.24±0.01	0.24±0.01	⋯	⋯

coefficients varying in the $(0.49-0.88)\times10^{-8}$ m^2 s^{-1} range for acetonitrile and $(0.65-2.3)\times10^{-8}$ m^2 s^{-1} range for carbon dioxide as x_{CO_2} is increased from the lowest to highest values.[11]

The D_t values calculated from the *NPT* and *NVT* simulations exhibit parallel variation with changes of CO_2 mole fraction, though the values at corresponding x_{CO_2} differ by more than their statistical errors. The differences may be explained by differences of liquid densities. Thus, in most cases, the *NPT* trajectories yield higher translational diffusion coefficients, as the simulated systems have underestimated densities. The only exception is pure CO_2, for which the *NPT* simulation overestimates the density and yields the higher D_t.

Molecular reorientations

The calculated values of the rotational correlation times are presented in Table III and Fig. 4. The experimental values for the pure liquids are $\tau=1.25$ ps for acetonitrile at 298 K and 1 bar,[29] and $\tau=0.27$ ps for carbon dioxide at 298 K and 68 bars.[30] Our calculations predict $\tau=1.13(3)$ ps (*NPT*, at 298 K and 1 bar) and 1.45(2) ps (*NVT*, 298 K and experimental 1 bar density) for pure acetonitrile, and $\tau=0.24(1)$ ps for pure CO_2 (both *NPT* at 298 K and 64 bars and *NVT* at 298 K and experimental 64 bar density). Thus, our calculated correlation times deviate by 5%–16% from measured values. This agreement is quite good for potentials that have not been specifically optimized for these properties.

As described in Methods, the correlation times τ are inversely proportional to rotational diffusion coefficients D_r. Thus, our simulation results show a clear trend for faster rotational diffusion of both carbon dioxide and acetonitrile components with rising CO_2 mole fraction. This trend parallels the behavior of the translational diffusion coefficients described above and may be analogously rationalized in terms of adding the more mobile CO_2 to the less mobile acetonitrile leading to slowing down of reorientations of the former while speeding up reorientations of the latter. The rate of reorientational motion in the mixtures may be varied by a factor of 2–3 by adjusting the amount of CO_2.

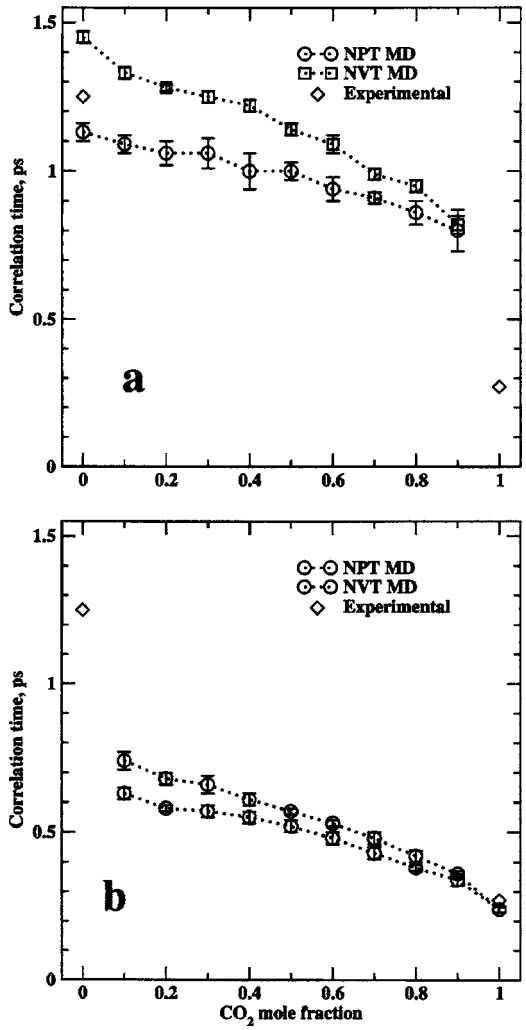

FIG. 4. Rotational correlation times in CO_2-acetonitrile mixtures. Units are ps=10^{-12} s. (a) Calculated values for acetonitrile: circles—*NPT*, squares—*NVT* MD. (b) Calculated values for CO_2: circles—*NPT*, squares—*NVT*. Diamonds: experimental values for pure acetonitrile at 1 bar and 298 K (Ref. 29) and for pure CO_2 at 64 atm and 298 K (Ref. 30).

The rotational correlation times calculated using the *NPT* and *NVT* methods show similar agreement with experimental data for the pure components and follow parallel trends of decreasing values with increasing x_{CO_2}. Thus, these approaches appear to be equivalent in terms of prediction of τ. Except for pure CO_2, the *NPT* values of τ are higher than the *NVT* results (corresponding to faster reorientation in the *NPT* trajectories). As in the case of translational diffusion, this trend may be explained by the tendency to underestimate the densities in the *NPT* simulations.

Shear viscosities

The calculated values of the shear viscosities η are presented in Table IV and Fig. 5. The measured value of viscosity of pure acetonitrile at 298 K and 1 bar is 0.341 cP (1 cP=10^{-3} Pa s).[16] The value calculated from our *NVT* simulation is 0.45(9) cP, overestimating the experimental result by 32%. For CO_2, the experimental value at 298 K and 64 bars is 0.057 cP, obtained from the formula defined by Eqs. (1), (3), (8) of Ref. 31. Our *NVT* simulations yield 0.059(3) cP for CO_2 at 298 K and its 64 bar experimental density. In this case the difference between experimental and calculated values is only 3%. Thus, our simulated viscosities of the pure components are in reasonable agreement with experimental data. This leads us to expect that we can reliably predict the viscosities of CO_2-acetonitrile liquid mixtures, with accuracy comparable to that achieved for the pure components.

TABLE IV. Shear viscosities of CO_2-acetonitrile mixtures calculated from *NVT* MD simulations. Units cP=10^{-3} Pa s. x is the CO_2 mole fraction.

x	η
0.00	0.448±0.087
0.20	0.287±0.036
0.40	0.248±0.033
0.60	0.190±0.031
0.80	0.116±0.040
1.00	0.059±0.004

The calculated viscosities of the mixtures exhibit a trend for systematic decrease with increasing x_{CO_2}. Changing from pure CH_3CN to pure CO_2 along the 298 K isotherm leads to a ca. eight-fold decrease of calculated viscosity; the experimental data give a six-fold decrease. Thus, the viscosity of the liquid phase can be manipulated over a relatively large range by expanding acetonitrile with compressed carbon dioxide. The results of Li and Maroncelli are similar, predicting a smooth variation of the liquid viscosity from 0.34 cP for pure acetonitrile to 0.079 cP for pure CO_2.[11]

DISCUSSION

Variation trends

The calculated transport properties show smooth, simple variation with composition, described by x, the mole fraction

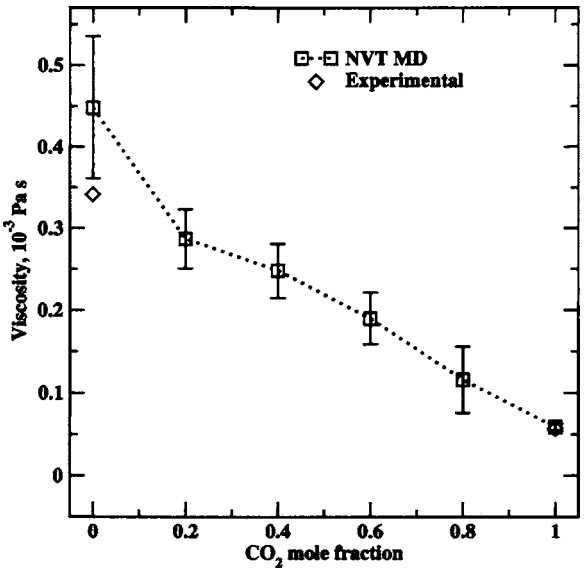

FIG. 5. Shear viscosity in CO_2-acetonitrile mixtures. Units are cP =10^{-3} Pa s. Calculated values for from *NVT* MD—squares. Experimental values of 0.341 cP for pure acetonitrile at 1 bar and 298 K (Ref. 16) and 0.057 cP for pure CO_2 64 atm and 298 K (Ref. 31) are marked by diamonds.

TABLE V. Coefficients for linear models for variation of transport properties with CO_2 mole fraction x. Units: Translational diffusion coefficients D_t in 10^{-8} m^2/s, rotational correlation times τ in ps, shear viscosity in cP $=10^{-3}$ Pa s. n—number of data points, $\chi^2=\Sigma_i[(y_i^{mod}-y_i^{obs})/\sigma_i]^2$, with σ as the reported errors from Table II–IV.

Property	Equation	a	b	n	χ^2
CH_3CN *NPT* translational diffusion coefficient D_t	$1/D_t=a+bx$	2.18	−1.20	10	1.5
CH_3CN *NVT* translational diffusion coefficient D_t	$1/D_t=a+bx$	2.96	−1.91	10	1.1
CO_2 *NPT* translational diffusion coefficient D_t	$1/D_t=a+bx$	1.62	−0.93	10	2.3
CO_2 *NVT* translational diffusion coefficient D_t	$1/D_t=a+bx$	2.18	−1.46	10	3.2
CH_3CN *NPT* rotational correlation time τ	$\tau=a+bx$	1.14	−0.34	10	0.5
CH_3CN *NVT* rotational correlation time τ	$\tau=a+bx$	1.43	−0.63	10	1.5
CO_2 *NPT* rotational correlation time τ	$\tau=a+bx$	0.69	−0.40	10	2.2
CO_2 *NVT* rotational correlation time τ	$\tau=a+bx$	0.81	−0.51	10	2.3
NVT shear viscosity η[a]	$\eta=a+bx$	0.34	−0.28	6	0.7
NVT shear viscosity η[b]	$\eta=a+bx$	0.45	−0.39	6	1.2

[a]Line through the two experimental data points for the pure liquids.
[b]Line through the two *NVT* calculated data points for the pure liquids.

of CO_2. The simplest correlations which could well represent the trends in the data are linear equations $(y=a+bx)$ for the rotational correlation time τ and shear viscosity η and inverse linear equations $(1/y=a+bx)$ for the translational diffusion coefficients. A summary of the fitting results is presented in Table V.

For translational diffusion coefficients, the inverse of D_t, which in our units roughly represents the average time in picoseconds needed for a molecule to move by 1 Å, decreases linearly with CO_2 mole fraction for both acetonitrile and carbon dioxide components.

For reorientational motions, the rotational correlation times τ for both components also decrease linearly with CO_2 mole fraction. In our units the correlation times roughly correspond to the average time in picoseconds for the molecular axis to reorient by 40°.

In the case of viscosity, straight lines drawn through the pure component data, either experimental or simulated, provide excellent models for variation with composition.

Hydrodynamic parameters

Hydrodynamic theory predicts that both translation and rotational diffusion rates should be inversely proportional to solvent viscosity. For a spherical particle under stick boundary conditions,

$$D_t = \frac{kT}{6\pi\eta a}$$

and

$$D_r = \frac{1}{6\tau} = \frac{kT}{6\eta V_h},$$

where k is the Boltzmann constant, T is the temperature, a is the particle radius, and V_h is its volume.[21,32] For nonspherical particles multiplicative correction factors may be found in the literature.[32] For particles of fixed shape and size, we expect that the reduced diffusion rates $D_t\eta$ and $6D_r\eta=\eta/\tau$ should remain constant at a constant temperature. The calculated reduced translational and rotational diffusion rates of both acetonitrile and carbon dioxide exhibit decreasing trends with rising CO_2 mole fraction (Fig. 6). This may be interpreted as the effect of increase of effective hydrodynamic sizes/volumes of both the components with increasing x_{CO_2}. A similar effect was found by Li and Maroncelli.[11] The explanation for these effects may be found in a detailed analysis of the local structure of the liquid mixture. This

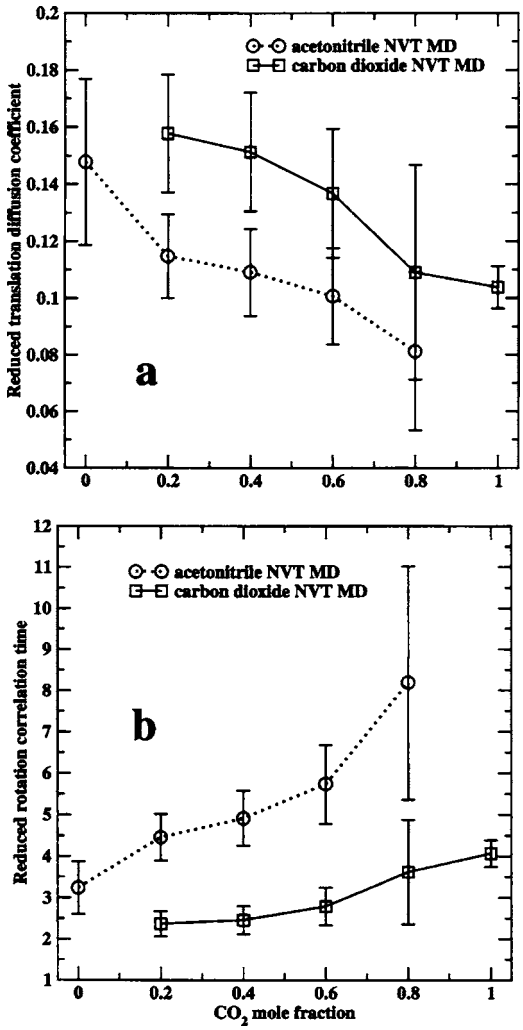

FIG. 6. Reduced transport coefficients in CO_2-acetonitrile mixtures. (a) Translational diffusion: $D_t\eta$ from *NVT* MD. Units are 10^{-11} N. (b) Rotational diffusion: τ/η from *NVT* MD. Units are 10^{-9} Pa^{-1}.

analysis will be part of a separate study of structure in CXLs which is under way at the CEBC and will be presented at a later date.

CONCLUSIONS

We present a molecular simulation study of the transport properties of liquid mixtures formed by acetonitrile and carbon dioxide, in which the CO_2 mole fraction is adjusted by changing the pressure, at a constant temperature of 298 K. We report values of translational diffusion coefficients, rotational correlation times and shear viscosities of the liquids as function of CO_2 mole fraction. We find that the calculated quantities exhibit smooth variation with composition which may be represented by simple model equations. The translational and rotational diffusion rates increase with CO_2 mole fraction for both the acetonitrile and carbon dioxide components. The shear viscosity decreases with increasing amount of CO_2, varying smoothly between the values of pure acetonitrile and pure carbon dioxide. Our results show that adjusting the amount of CO_2 in the mixture allows the variation of transport rates by a factor of 3–4 and the variation of liquid viscosity between pure acetonitrile and pure carbon dioxide values. Thus, the physical properties of CO_2-expanded acetonitrile may be tailored over a wide range by changes in the operating conditions of temperature and pressure.

Our calculations provide predictions of transport properties of CO_2-expanded acetonitrile, for which experimental data are lacking. Using potential energy functions taken from the literature, we have been able to reproduce the available experimental data for the pure components quite well. Thus we believe that our calculations also provide reliable, though approximate, results for the unknown properties of the mixtures. Additionally, the simulations provide insights into the microscopic properties of the mixtures. Thus, we found that transport rates tended to vary faster with composition than expected from calculated viscosities. This suggests that hydrodynamic parameters of the molecules change with composition. Our studies of the CO_2-acetonitrile mixtures provide important new information about the properties of this class of liquids and of CXLs in general. Studies of transport and structure in a variety of CXL systems will be the topic of our future studies.

ACKNOWLEDGMENT

This work was supported by National Science Foundation Grant No. ERC-0310689 providing for the Center for Environmentally Beneficial Catalysis at the University of Kansas.

[1] J. M. DeSimone, Science **297**, 799 (2002).
[2] P. G. Jessop, D. Heldebrant, X. Li, C. Eckert, and C. L. Liotta, Nature (London) **436**, 1102 (2005).
[3] P. Licence and M. Poliakoff, in *Multiphase Homogeneous Catalysis*, edited by B. Cornils (Wiley-VCH, Weinheim, 2005), p. 734.
[4] H. Jin and B. Subramaniam, Chem. Eng. Sci. **59**, 4887 (2004).
[5] C. Lyon, V. Sarsani, and B. Subramaniam, Ind. Eng. Chem. Res. **43**, 4809 (2004).
[6] B. Rajagopalan, M. Wei, G. Musie, B. Subramaniam, and D. Busch, Ind. Eng. Chem. Res. **42**, 6505 (2003).
[7] B. Subramaniam and D. H. Busch, in *Use of Dense-Phase Carbon Dioxide in Catalysis*, ACS Symposium Series No. 809, CO2 Conversion and Utilization, edited by A. M. G. C. Song and K. Fujimoto, p. 364 (American Chemical Society, Washington, 2002).
[8] Y. Houndonougbo, H. Jiu, B. Rajagopalan, K. Wong, K. Kuczera, B. Subramaniam, and B. B. Laird, J. Phys. Chem. B **110**, 13195 (2006).
[9] J. Harris and K. Yung, J. Phys. Chem. **99**, 12021 (1995).
[10] Y. Hirata, J. Phys. Chem. A **106**, 2187 (2002).
[11] H. Li and M. Maroncelli, J. Phys. Chem. B **110**, 21189 (2006).
[12] I. Suzuki, J. Mol. Spectrosc. **25**, 479 (1968).
[13] B. R. Brooks, R. Bruccolleri, B. Olafson, D. States, S. Swaminathan, and M. Karplus, J. Comput. Chem. **4**, 187 (1983).
[14] J. P. Ryckaert, G. Ciccotti, and H. J. C. Berendsen, J. Comput. Phys. **23**, 327 (1977).
[15] R. Amadera and S. Krimm, Spectrochim. Acta, Part A **24**, 1677 (1968).
[16] *CRC Hand Book of Chemistry and Physics*, 81st ed. edited by R. Weast (CRC, Cleveland, OH, 2001).
[17] A. Kordikowski, P. Schenk, A. R. M. Van Nielen, and C. J. Pieters, J. Supercrit. Fluids **8**, 205 (1995).
[18] M. P. Allen and D. J. Tildesley, *Computer Simulations of Liquids* (Oxford Science, London, 1987).
[19] S. E. Feller, Y. Zhang, and R. W. Pastor, J. Chem. Phys. **103**, 4613 (1995).
[20] C. Sagui and T. A. Darden, Annu. Rev. Biophys. Biomol. Struct. **28**, 155 (1999).
[21] D. A. McQuarrie, *Statistical Mechanics* (Harper & Row, New York, 1976).
[22] M. Ehrenberg and R. Rigler, Chem. Phys. Lett. **14**, 539 (1972).
[23] T. J. Chuang and K. B. Eisenthal, J. Chem. Phys. **57**, 5094 (1972).
[24] J. M. Haile, *Molecular Dynamics Simulation* (Wiley-Interscience, New York, 1992).
[25] D. M. Newitt, M. U. Pai, N. R. Kuloor, and J. A. W. Huggill, in *Thermodynamic Functions of Gases*, edited by F. Dim (Butterworth, London, 1956), Vol. 123.
[26] N. B. Vargaftik, *Handbook of Physical Properties of Liquids and Gases: Pure Substances and Mixtures*, 3rd Augmented and Revised Edition (Begell House, New York, 1996).
[27] R. L. Hurle and L. A. Woolf, J. Chem. Soc., Faraday Trans. 1 **78**, 2233 (1982).
[28] P. Etesse, J. A. Zega, and R. Kobayashi, J. Chem. Phys. **97**, 2022 (1992).
[29] C. Wakai, H. Saito, N. Matubayashi, and M. Nakahara, J. Chem. Phys. **112**, 1462 (2000).
[30] T. Umecky, M. Kanakubo, and Y. Ikushima, J. Phys. Chem. B **107**, 12003 (2003).
[31] A. Fenghour, W. A. Wakenham, and V. Vesovic, J. Phys. Chem. Ref. Data **27**, 31 (1998).
[32] C. R. Cantor and P. Schimmel, *Biophysical Chemistry, Techniques for the Study of Biological Structure and Function* (Freeman, New York, 1980), Vol. II.